A Determination of the Strengths of the Sporadic Radio-Meteor Sources.

P. Brown and J. Jones
Department of Physics, University of Western Ontario, London, Ont., N6A 3K7, Canada

Presented at the *International Conference on Meteoroids 28-31 August 1994 in Bratislava.*

Submitted to "*Earth, Moon and Planets*"

Please address all communication concerning this paper to

Mr P. Brown
Physics Department,
University of Western Ontario,
London, Ontario.,
CANADA N6A 3K7

224

Abstract

We have calculated the response functions for the Springhill (Ottawa) and Christchurch (New Zealand) radars. Using the sizes and locations of each of the six sporadic radio-meteor sources found in our previous study (Jones and Brown, 1993), we have determined the response of each radar to each of the sources. Then, using least-squares fit to data collected over several years, we have determined the strength of each source. Excellent agreement with the non-radar data is obtained for the total flux after application of a correction for the initial train radius. The results from the two radars show good consistency for the sources which are visible to both of them. For individual years the fits are good to between 5 and 10% but there does appear to be some variability from year to year which may be due to atmospheric effects.

1. Introduction

In a previous work the authors (Jones and Brown, 1993) (hereafter JB) developed an empirical model for the distribution of sporadic meteor radiants over the celestial sphere based on data from orbital radar surveys. That work was a continuation of modelling started by the first radar surveys of sporadic radiants by Hawkins(1957) and later by Elford et al. (1964) and Stohl (1968). These works have shown that the sporadic complex observed froim the Earth is not isotropic, but rather shows major concentrations of radiants distributed symmetrically about the celestial sphere when viewed in sun-centred coordinates.The six major sources found by JB are shown in Figure 1.
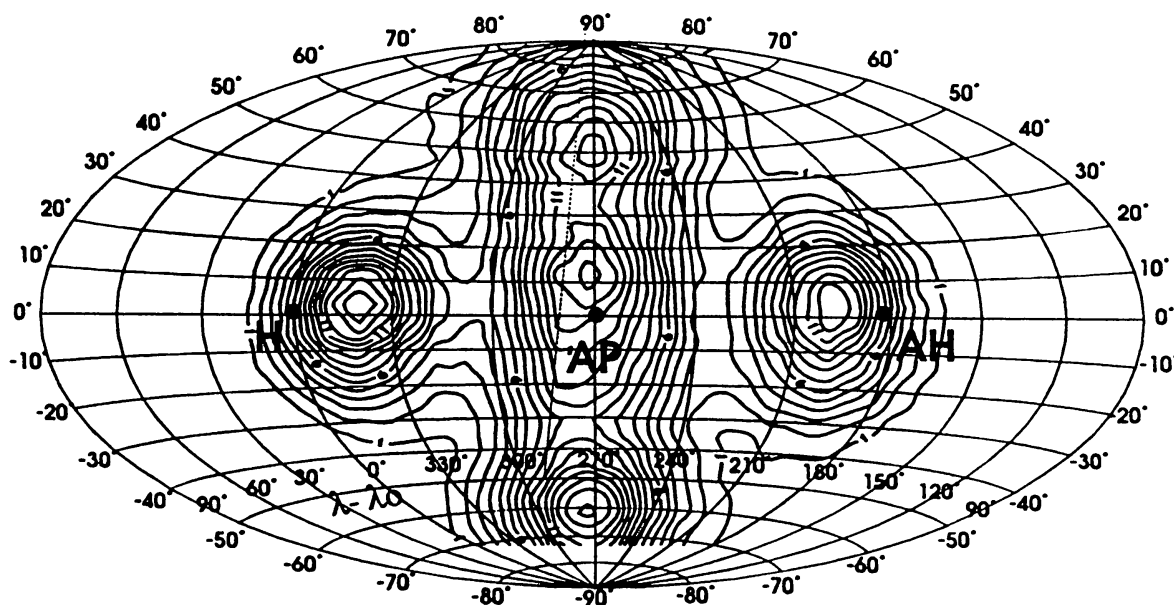

Figure 1. Contour plot of monte carlo generated sporadic meteor radiants using the source characteristics found in Jones and Brown (1993). The asymmetry in the apex sources results from the poorly defined characteristics of the south apex source.

They are designated as the Helion and Anti-Helion sources which have radiant areas near the solar position in the sky and opposite the helion point, the North and South Apex sources which have radiant areas that straddle the Apex of the Earth's way and the North and South Toroidal sources

which have high ecliptic latitude radiants and are so named because their high inclinations produce a group of orbits which resemble a Toroid about the Earth's orbit. While our earlier work was able to describe some of the physical properties of these sources such as radii and location, the mean strength of the sources remained undetermined.

To accomplish this goal we have chosen meteor echo data collected at two radar sites: one in Springhill (near Ottawa), Canada and the other in Christchurch, New Zealand. Both of these systems were patrol in nature; they operated nearly continuously for several years with precisely the same equipment setup so rate variations can be related most probably to true variations in the flux of meteoroids. The Springhill system worked at 32.7 MHz with a peak power of 20 KW and showed mean hourly meteor echo rates from 100-300. The limiting sensitivity of the system was near visual magnitude +7. The Christchurch radar operated at 69.5 MHz having a peak power of 81 KW and recorded mean meteor echo rates typically in the range of 100-200 with a sensitivity approaching +9 Mv. More details of the systems can be found in Neale (1966), Millman and McIntosh (1964, 1966) for Springhill and Ellyett and Keay (1963) for the Christchurch system. To use the data, we must choose for the data bins some widths which are statistically meaningful. We did so by having the total number of echoes recorded from each system binned into 2-hour averages for each month during the year. The two hour bins provide an acceptable compromise between minimizing short term increases in flux caused by showers without masking the diurnal variation in sporadic activity. Such a method is justified in view of the smooth variation and long-time scales involved in sporadic activity changes, both diurnally and annually. Though this procedure minimizes the effects of streams, some of the stronger ones still affect the data.

Table 1.

Source	AH	H	NT	ST	NA	SA
Position	198,0	342,1	271,58	274,-60	271,19	273,-11
Radii	18	16	19	16	21	-

Table 1. Mean source characteristics as derived in the study of Jones and Brown (1993). Abbreviations stand for: AH - Anti-Helion source, H- Helion source, NA- North Apex source, SA - South Apex source, NT- North Toroidal and St - South Toroidal source. For more details see JB.

Taking the results from JB for the six different sources and the associated mean radii of each source (table 1), we generated a model distribution of individual sporadic meteor radiants. Specifically, 1000 sporadic radiants were chosen for each source, centred at the appropriate mean source location given in table 1. The radiants were generated in a monte carlo procedure using a probability function of the form:

$$P(\theta-\theta_o)=\exp[\frac{-\ln(2)(1-\cos(\theta))}{1-\cos(\theta_o)}] \tag{1.1}$$

where θ is the angular distance from the centre of the distribution and θ_o is the mean radii of the source. This distribution was chosen on empirical grounds alone as it reproduced well the physical character of the sources as seen from the surveys and because it behaved well numerically. Figure 1

226

shows the resulting theoretical distribution. Note that since the amount of data available from the southern hemisphere is much less than in the northern hemisphere, the characteristics of the South Apex source are very uncertain and a direct application of the observed physical attributes as performed here yields a South Apex source shifted considerably closer to the ecliptic plane than its northern counterpart. Such factors account for the apparent assymmetry near the Apex.

Having developed a representative model distribution, we next use it to interpret the echo data, noting that these are given as the number of meteors detected by the system per unit time. By taking the model radiant distribution and calculating the effective collecting area of each source for a given radar we can then perform a least-squares fit on the actual data using the model data as input. The coefficients in this expansion then represent the mean strength for each source throughout the year in units of flux. The degree to which the fits match the actual echo data and the derived fluxes match flux distributions found from other studies will help determine if the model is realistic.

2 Theoretical Considerations

The echo rate detected by radar is a function of the flux of meteoroids incident over the Earth's surface multiplied by the effective collecting area of the radar. Mathematically we can represent the echo rate by the equation (Kaiser, 1960):

$$\Psi(t) = \int\int \Phi(\alpha,\delta)\Theta(\alpha,\delta,t)d\Omega \qquad (2.1)$$

where $\Theta(\alpha,\delta,t)$ is the flux from a radiant in the (α,δ) direction and $\Phi(\alpha,\delta)$ is the effective collecting area of the radar system from the same radiant.

Since we know the echo rate, $\Psi(t)$, we need merely find the effective collecting area, $\Phi(\alpha,\delta)$, to determine uniquely the flux, $\Theta(\alpha,\delta,t)$. The collecting area for a given system is found by using the aspect sensitivity inherent in the scattering process and knowledge of the gain pattern for a given system. We may then find $\Theta(\alpha,\delta,t)$. To simplify the problem, we make use of the fact that there are only 6 significant sources of sporadic activity over the celestial sphere and turn the integral in Equation 2.1 into a discrete sum of six sources whose collecting areas can be found. By performing a least squares fit to the rate data we can then find a mean source strength (and hence flux) associated with each source region. For the purposes of simplicity we take the sources to have constant widths, constant locations, one constant strength throughout the year and to be comprised of a similar particle size-distribution unchanging throughout the year. In reality, some or all of these physical characteristics may change on an annual basis, but the problem becomes strongly non-linear and much more difficult to handle if we attempt to take these as free parameters and it is not clear that we would thereby gain any additional insight into the processes involved or be able to increase the precision of our final answer.

2.1 Calculation of the Collecting Area

The general method for calculation of collecting areas has been presented in several past works (cf. Kaiser, 1960). We have used these methods as a guide for the present technique and present it in detail here so that it might be useful for other workers.

To calculate the collecting area for a system we must determine the total area in the atmosphere over which the radar is sensitive for a given radiant. Each underdense meteor trail

displays aspect sensitivity insofar as radio wave reflection is possible only when the trail is oriented perpendicular to the radar line of sight.

To visualize the method of determining the collecting area we may first construct an "echo-line" by taking dh →0 in figure 2. All meteor trails detected from a given radiant will cross this echo-line. The echo-line is the intersection of the plane which contains the radar at R and whose normal lies in the direction of the radiant, **m,** and the height at which ablation occurs (typically ~100 km). If **n** is the unit vector radially outward from the transmitter, then via the specular reflection condition it can also be described by the equation **m.n**=0.
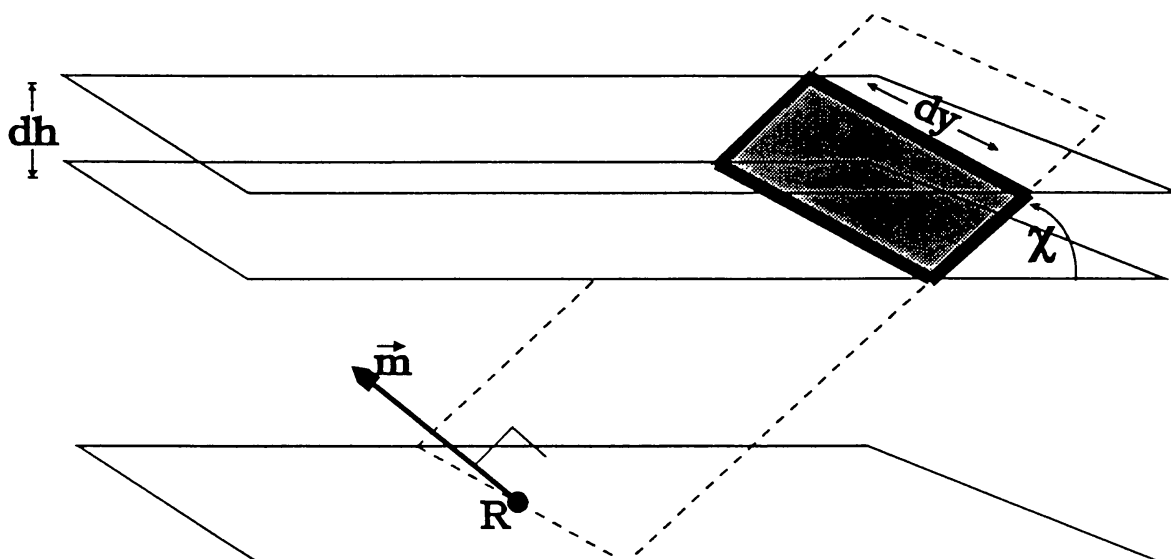

Figure 2. Geometry of the echo-strip (shaded region). Here R refers to the radar site, m is the direction to the radiant from the radar, dh is the height interval overwhich ablation occurs (see Figure 3) , and χ is the zenith angle of the radiant. dy reperesents the transverse distance along the echo-strip. The dotted plane is perpendicular to the radiant direction.

If the meteors occurred at one discrete height only this would be an accurate representation; in fact the ablation process extends over about 5 kilometres of altitude in the atmosphere. As a result, the echo-line is really a strip and it is the area of this strip which we call collecting area. A unit of area, **da,** along the echo-strip is given by:

$$da = \frac{dh \, dy}{\sin(\chi)} \frac{m}{|m|}$$ (2.1.1)

where dh is the mean vertical trail length of the meteor appropriate to the particle population being considered, χ is the zenith angle of the meteor radiant and dy is distance along the echo-strip.

To determine the mean vertical trail length we could appeal to classical meteor ablation theory as previous workers have for collecting area calculations, but in this case we would have to ignore processes such as fragmentation. Instead, we choose to use empirical results of mean vertical trail lengths gathered from Low-Light-Level TV observations of faint meteors (limiting sensitivity of about +7), which cover the same particle population as in radio studies. Such an analysis has recently been presented by Flemming, Hawkes and Jones (1993). Figure 3 presents the final result of their work relating the mean vertical trail length to the mass index, s. A reasonable value for s has been found to be roughly 2 for the sporadic background (cf. Kaiser (1954), Babadzhanov (1992)) while it is usually somewhat less for shower meteors (Webster, Poole and Kaiser (1966), McKinley (1961)).
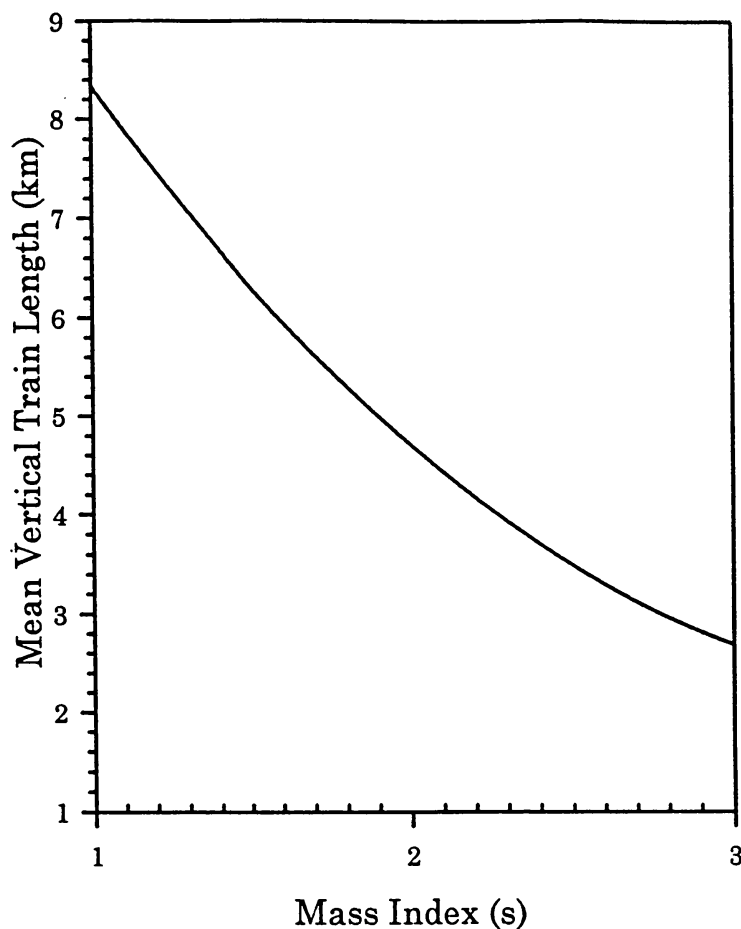

Figure 3. Mean vertical length of meteor trains as derived from the low-light-level observations of Flemming, Hawkes and Jones (1993).

Next, we must calculate the antenna gain pattern for the systems in question. In the present work, we are concerned with calculating the collecting area for the radar systems at Christchurch and Springhill, both of which use a crossed-dipole antenna fed in quadrature. Note that as we are concerned with the relative gain only we reference each gain pattern to the nominal zenithal value and refer to it as g(x,y). The (x,y) dependence refers to the location of the echo point in (x,y,z)

coordinates with z=100km being the mean height of the echo region and x,y the position of the trail echo point projected onto the ground; in this system the radar is at (0,0,0).

To calculate the total effective collecting area for a given radiant we write:

$$\Phi(\alpha_m, \delta_m) = \int (g(x,y)\sec\chi)^{s-1} da \qquad (2.1.2)$$

where the subscripts remind us that the integration is for a particular radiant. Both g(x,y) and sec(χ) are weighting terms to take into account, respectively, the reduction in collecting efficiency when the detection direction is away from the main antenna gain beam or when the radiant is low and the ionization is spread over a longer path reducing the line density. The exponent on this relative gain function takes into account the fact that all echoes with line densities greater than the minimum line density detectable at the zenith are counted in accordance with the cumulative flux power-law. It is these weighting terms that yield an "effective" collecting area from equation 2.1.2 as opposed to a simple geometrical collecting area which would be found by simply integrating da.

For the systems considered here, the gain patterns show variations in sensitivity solely as a function of elevation, they are effectively azimuthally symmetric; as a result the echo collecting areas are purely functions of the altitude of the radiant. Figures 4 and 5 show the calculated collecting area for both the Christchurch and Springhill systems for various mass indices, respectively. The sharp cutoff for Springhill at a radiant altitude of 75° reflects the fact that no echoes beyond a slant range of 370km were counted in the final statistics (McIntosh, 1966). The shape of the collecting area functions for Springhill compare well with those calculated by McIntosh (1966).
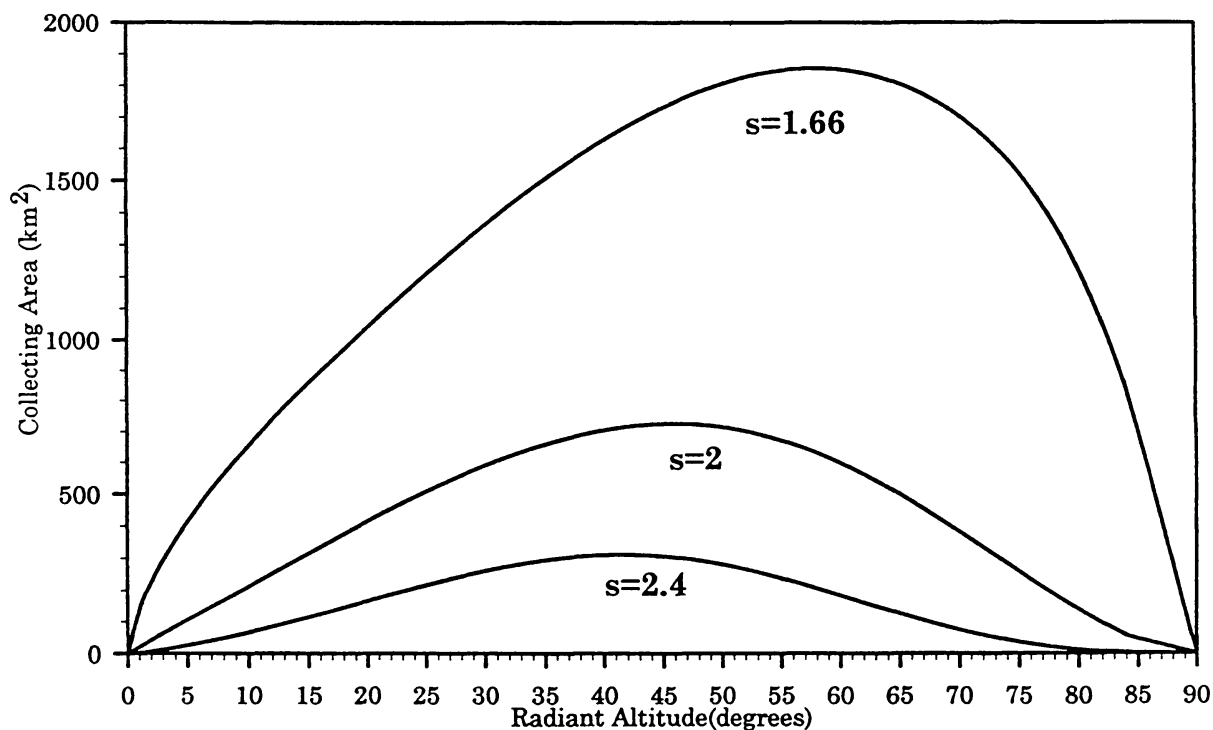

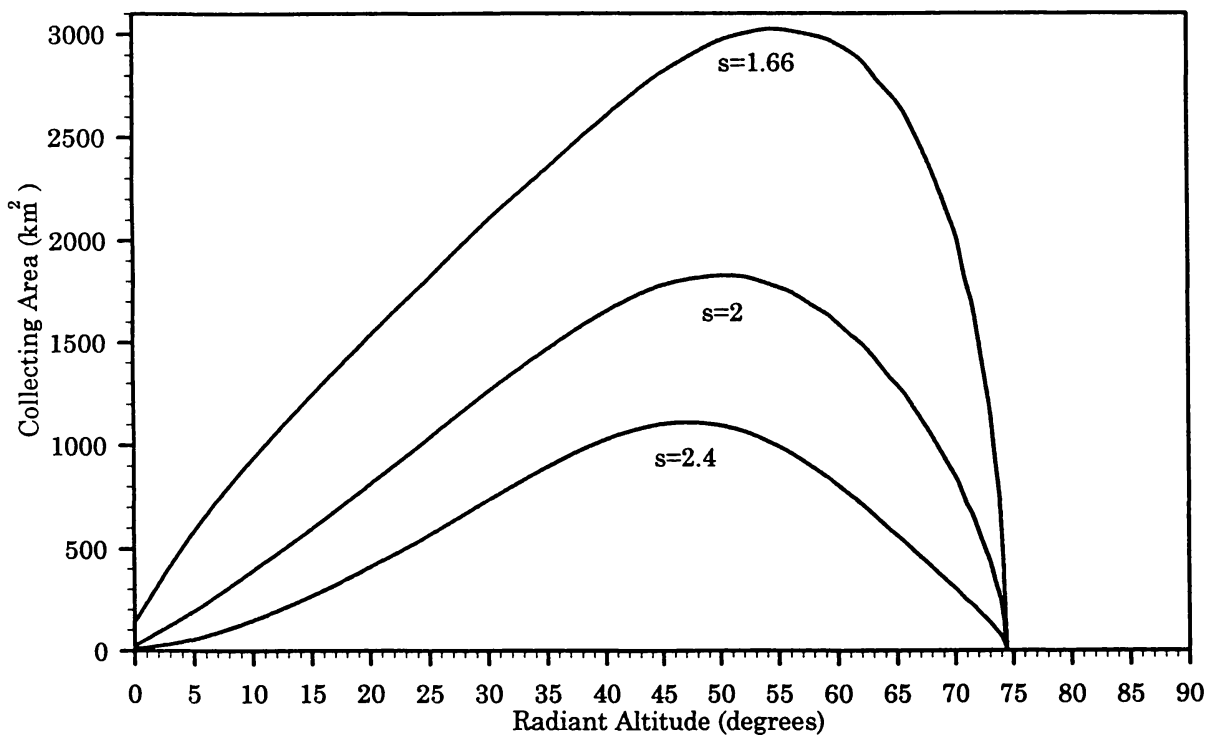Figure 4. Collecting area as a function of radiant altitude for Christchurch for three values of the mass index, s.

230

Figure 5. Collecting area as a function of radiant altitude for Springhill for three values of the mass index, s.

3 . Results

After generating the model sporadic radiant distributions and determining the collecting area we were able to use the rate data in an annual format to perform a simple least-squares fit on the model radiant distribution.In this scheme, the radiant sources form a basis which we can then use to fit the observed rates. We can express the theoretical rates, $Th_{rate}(t)$, by an equation of the form:

$$Th_{rate}(t) = \sum \mu_i S_i \tag{3.1}$$

where μ_i represent the source strengths (in units of flux) and S_i represents the collecting area appropriate to a given source at time t. The source strengths are fit to the entire year's worth of rate data so that we get one set of strengths for each year. The collecting area appropriate to each source was found by calculating the average collecting area as a function of time for the distribution of sporadic radiants specific to those sources given by equation 1.1.

The results of two typical fits are presented in figures 6-7. The top contour rate diagram for each figure represents the observed rate pattern throughout the year while the bottom diagram represents the least-squares fit. As previously mentioned, the binning chosen eliminated all but the strongest annual showers in that the bins are large enough in time (a month) to average out the effects of moderate, but short-lived increases in rates due to most showers. To ensure that the source

Figure 6. Meteor rate data (top) for Christchurch in 1960. The bottom plot shows the fit to the data using the empirical sporadic radiant model and including contributions from the Delta Aquaruids, Geminids and a radiant at (210,-5) in sun-centred coördinates in mid-December.
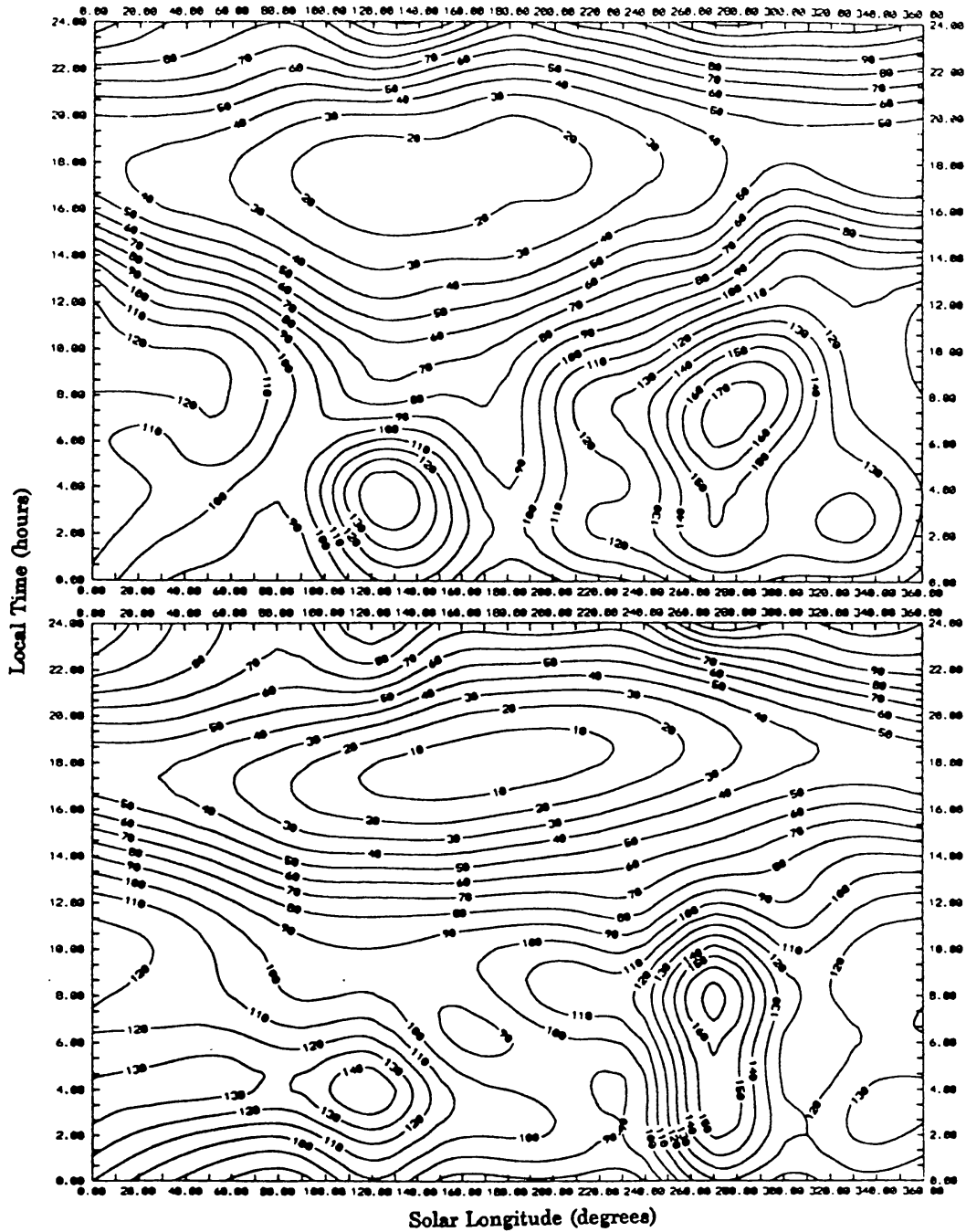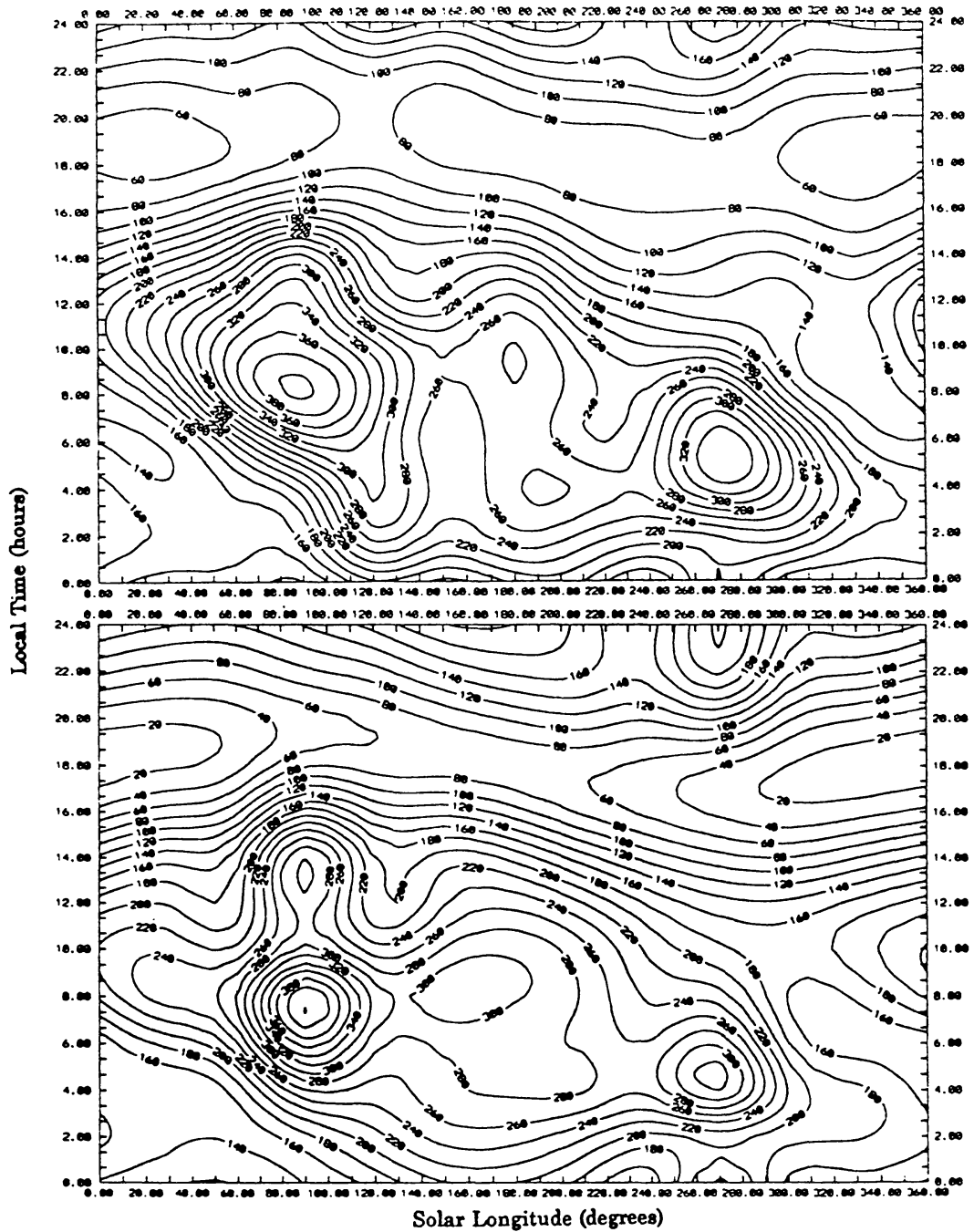
232

Figure 7. Meteor rate data (top) for Springhill in 1965. The bottom plot shows the fit to the data using the sporadic radiant model and including contributions from the Zeta Perseids and the Geminids.

strengths found from the least-squares fit accurately represented the sporadic background we masked the showers obviously present in a given years data by including that shower as a separate source along with the sporadic sources in the fitting routine. As a result, the activity from the shower does not affect the value of the least-squares coefficient appropriate to the sporadic sources. For this work we define a sporadic meteor as one which does not belong to any one of the dozen strongest showers throughout the year. We use this definition for pragmatic reasons and do not wish to imply that sporadic meteors have any special origin or history. As such, the sporadic background investigated here undoubtedly still includes numerous minor showers.

In general, considering the simple model employed to represent the sporadic background, the fits are remarkably good. Typically, all regions are matched to better than 10% of the observed rates and most are better than 5%. The diurnal characteristics are correct in that a low rate is seen from each location near 18h local time with peak rates in the early morning hours (roughly 06h local) in agreement with other studies, employing radio, visual and photographic methods (Lovell (1954), McKinley (1961), Millman and McIntosh (1963), Vogan and Campbell (1957), Stohl (1968) and more recently in Mawrey and Broadhurst (1993)). The effects of showers as intensely localised (both diurnally and seasonally) increases in rates are apparent from both sites.

Specifically, the Springhill data are heavily contaminated in June ($\lambda \sim 90°$) by the daytime Arietid-ζ Perseid complex of streams. These are known to be the strongest radio streams, being among the first ever recorded by radar methods (Almond, 1951). Lesser contamination also occurs for the Geminids, Orionids, and Perseids. Very intense and short-lived activity from the Leonids is also apparent in 1966 and to a lesser degree in 1965 as a result of meteor storm outbursts.

The Christchurch data suffer principally from a shower with activity in December/January found to have a radiant near (210,-5). Note that this radiant was found purely by trial and error, in an attempt to fit the observed rate patterns with an appropriate collecting function and may represent activity from any one of the ecliptic showers active at that time. Other studies have suggested this to be activity related to several small streams called the Vela-Puppid complex (Ellyett et al., 1961). Lesser contamination occurs for the δ-Aquarids in July and Geminids in December for Christchurch.

3.1 Flux Estimates

By taking the source strengths given in table 2, found by fitting the model to the data, we can derive absolute fluxes of meteoroids reaching the Earth and perform another check on the acceptability of the sporadic radiant model.

In doing so two key parameters must be defined:

(1) The limiting size of meteoroid visible to the radar.
(2) The total true flux at that meteoroid size.

To define (1) for the Christchurch and Springhill system, we found the minimum detectable power by assuming the receivers were near optimal in design so that the receiver noise could be found from the system bandwidth,. The minimum detectable line density was then taken as 10 db above noise level (cf. Keay, 1963). The minimum detectable line density as a function of altitude are given in figure 8. The radio magnitude is defined as (McKinley, 1961):

$$M_r = 40 - 2.5\log(\alpha) \qquad (3.2.1.)$$

234

Table 2.

Radar	Year	AH	±AH	H	±H	NT	±NT	ST	±ST
Christchurch	1960	9.04	0.55	7.59	0.70	·	·	4.91	0.31
	1963	15.9	1.2	12.0	1.2	·	·	4.09	0.56
	1964	12.7	0.76	9.73	0.93	·	·	3.96	0.37
Springhill	1959	9.27	0.58	7.17	0.57	3.26	0.34	·	·
	1960	10.4	0.66	6.35	0.66	5.09	0.39	·	·
	1963	8.98	0.65	10.7	0.70	5.4	0.38	·	·
	1964	11.0	0.57	13.3	0.56	4.29	0.33	·	·
	1965	8.61	0.48	10.7	0.48	3.36	0.25	·	·
	1966	10.7	2.00	13.5	0.8	4.72	0.52	·	·
	1967	12.0	0.68	12.8	0.8	5.94	0.41	·	·

Radar	Year	NA	±NA	SA	±SA	Total Flux	σ^2
Christchurch	1960	·	·	7.87	0.21	7.35	13.5
	1963	·	·	12.3	0.57	11.1	28.9
	1964	0.05	0.42	9.51	0.67	9.0	19.0
Springhill	1959	·	·	10.5	0.2	7.56	38.3
	1960	·	·	7.59	0.1	7.35	44.1
	1963	·	·	14.3	0.2	9.87	46.6
	1964	2.29	0.44	5.6	0.2	8.54	37.5
	1965	0.11	0.10	7.36	0.1	7.54	32
	1966	·	·	13.3	0.63	10.5	43.1
	1967	·	·	16.2	0.22	11.8	51.6

Table 2. Corrected flux values by source for each year data was avaliable for Christchurch and Springhill for the empirical sporadic source model. All fluxes are given in units of 10^{-2} km^{-2} hr^{-1}. The σ^2 column is the rms variation of the fitted rates relative to the observed rate data in units of meteors hr^{-1}. The columns headed by ± represent the error associated with the flux from a given source. The total flux is the sum of each source flux divided by four to account for the directional nature of the fluences (see text).
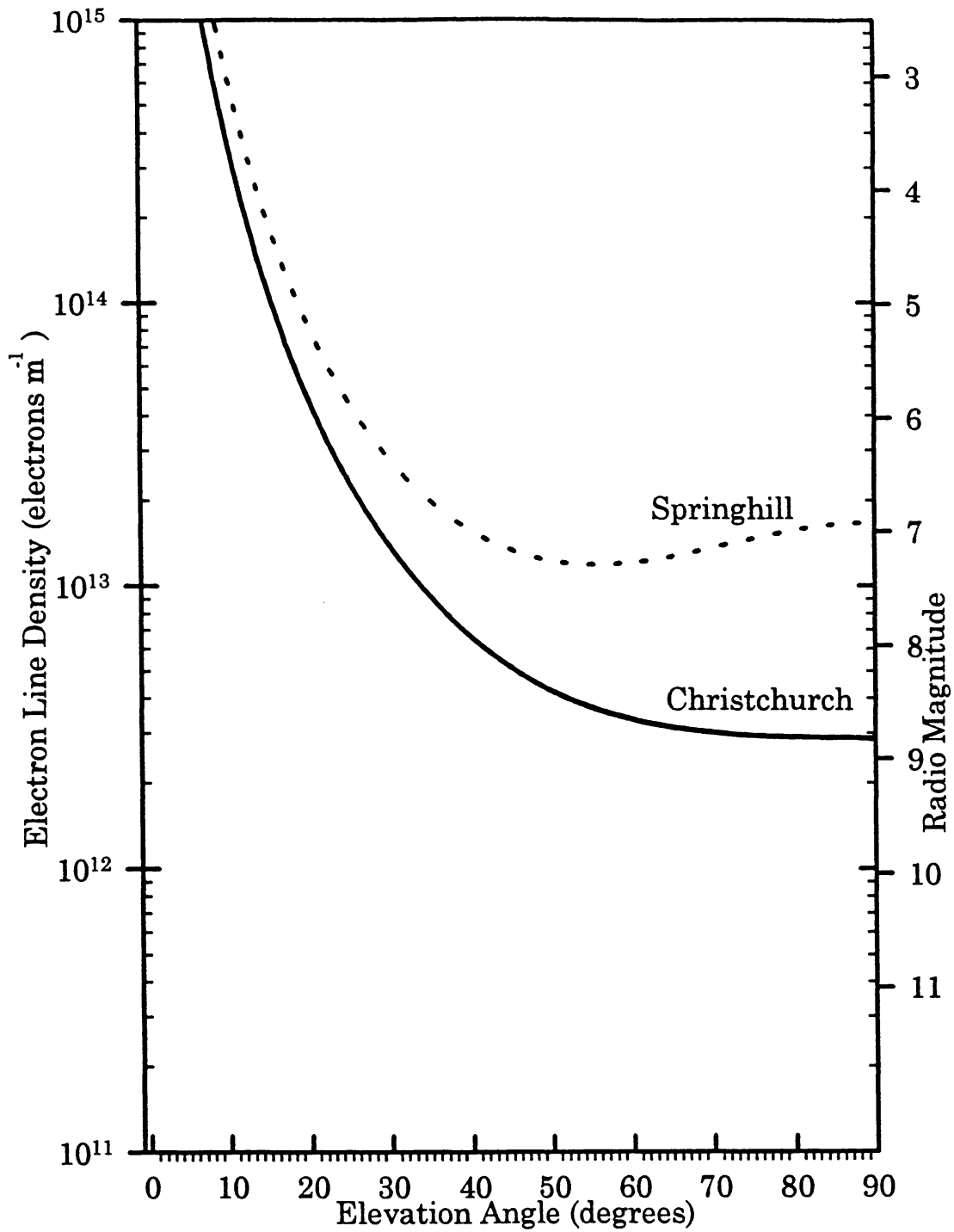
Figure 8. Minimum detectable electron line densities as a function of altitude for Springhill and Christchurch. Note the small dip in the Springhill pattern far from the zenith caused by the larger lobes for Springhill.

This relation has been derived from simultaneous visual and radio echo observations and is equivalent to absolute visual magnitude. Recall that each radar system is referenced to the zenithal gain, hence the line density overhead (essentially a minimum in both cases) is the system limiting line density for our purposes and corresponds to $M_r \sim 6.8$ for Springhill and $M_r \sim 8.6$ for Christchurch. These values are in general agreement with those derived for the same systems by McIntosh and Simek (1980) as $\sim +7$, and $+8.2$ for Christchurch (Elford, 1967).

To determine the true absolute flux from the values given by the source strength (the source strengths are really apparent fluxes), we must ensure that all meteors of this limiting magnitude and brighter are included in the cumulative sum. One important observational bias in this regard is connected with the initial train radius. Recent work has shown this effect to be very significant for radars operating above ~ 10 MHz (Olsson-Steel and Elford, 1986) as the true height distribution of meteors peaks near ~ 140km, while conventional radars, in comparison, show peaks from 90-100km depending on wavelength.

This bias was first recognized by Greenhow and Hall (1960), who studied the effect quantitatively by looking at the height distribution for 3 identical radar systems operating at different wavelengths and showed it is possible to derive the total fraction of meteors detectable at any wavelength. A further refinement to the procedure was made by Jones (1983) who included the effect of differing minimum detectable masses using the radar systems of Greenhow and Hall as references. By applying the corrections from Greenhow and Hall and the additional small correction from Jones we can define the fraction of meteors actually detected by a system. Unfortunately, the details given in Greenhow and Hall do not allow estimation of the errors involved in this treatment.

This analysis was performed for Springhill and Christchurch where 12% and 1% of the total meteor flux respectively is actually detected. For comparisons with other meteor radar data, similar corrections were applied to published data where limiting line densities and total fluxes were given. Note that to derive apparent fluxes, each author has chosen an appropriate sporadic radiant distribution model. For all systems listed, with the exception of Kharkov, the sporadic flux models were early versions of the present model, generally based on the work of either Hawkins (1956) or Elford et al. (1964). We note, however, that while these generally produce poorer fits to long-term rate data, the Hawkins' model incorporates the AH and H sources which account for 2/3 of the sporadic flux, so that the final derived total average fluxes are similar to those found from the sporadic model developed in JB.

The radar systems used and the resultant corrected sporadic fluxes are listed in table 3. To assess the flux curve derived from the radio data for meteoroids over the magnitude range M_r $6.8 < 15.3$ given in the table, we compared model meteoroid flux distributions derived from spacecraft dust detection experiments, zodiacal light measurements and impact studies with the individual radar data points. The data are from Grün et al.(1985). These sources list fluxes as a function of mass - hence a conversion is needed to equivalent magnitude as the meteoroids would appear in the atmosphere. In all cases a mean sporadic velocity of 40 km/s - 30 km/s was assumed in accordance with other work (Thomas and Whitham, 1988, Lovell, 1952) and the magnitude mass relation of Verniani (1973) derived from data in the magnitude range $6 < M_r < 10$ was used. In fact, this relationship between magnitude and mass seems valid over a wide range (cf. Jacchia et al., 1965 for $-4 < M_r < 2$ and Duffy et al., 1988 for $3 < M_r < 6$ which are all very similar).

Table 3.

Radar	$\lambda_{true}(m)$	$\lambda_{eff}(m)$	$\Theta_{observed}$ $(km^{-2}hr^{-1})$	$\Theta_{corrected}$ $(km^{-2}hr^{-1})$	Limiting Mag
Christchurch	4.32	3.85	0.0912	8.9	8.6
Springhill	9.17	10.0	0.0902	0.7	6.8
Harvard	7.30	3.87	10	893	13.4
Kharkov	8.00	6.19	3.63	89	10
Jindalee	30.00	13.58	376	1555	15.3
Elginfield	6.00	7.36	0.0316	0.52	6.7

Radar	Year	NA	±NA	SA	±SA	Total Flux	σ^2
Christchurch	1960	1.20	0.15	6.87	0.35	7.28	13.6
	1963	0.04	0.26	11.9	0.78	10.77	28.5
	1964	1.73	0.17	8.06	0.51	8.9	18.6
Springhill	1959	0.56	0.20	10.2	0.18	7.84	37.7
	1960	1.23	0.24	6.47	0.2	7.47	44.2
	1963	0.21	0.30	14.5	0.05	10.37	45.1
	1964	3.39	0.20	2.13	0.17	8.48	37.2
	1965	1.96	0.17	5.58	0.15	7.64	32.3
	1966	0.71	0.07	12.8	0.66	10.94	42.6
	1967	-	-	17.2	0.22	12.3	58.7

Table 3. Corrected sporadic flux for selected radars. The values for Christchurch and Springhill were derived from this work, for Harvard from Elford et al. (1964), for Kharkov from Lebedinets (1964), for Jindalee from Thomas et al. (1988) and from Elginfield from Jones and Webster (1992). The Super-Schmidt flux is from Hawkins and Upton (1958) while the visual flux is from Millman (1957).

Under this mean velocity assumption, the uncorrected radio meteor flux and the fluxes determined by other means are given in figure 9. There is quite poor agreement between the interplanetary flux models and the uncorrected rate data. Note that the points for Christchurch and Springhill derived from this work represent the average summed source strengths over all years where observations were available. The errors for these two points are the same size as the symbols. For comparison, the corrected fluxes are show in figure 10. Here an excellent degree of similarity exists between the two sets of data and suggests the initial train radius corrections applied, transform the
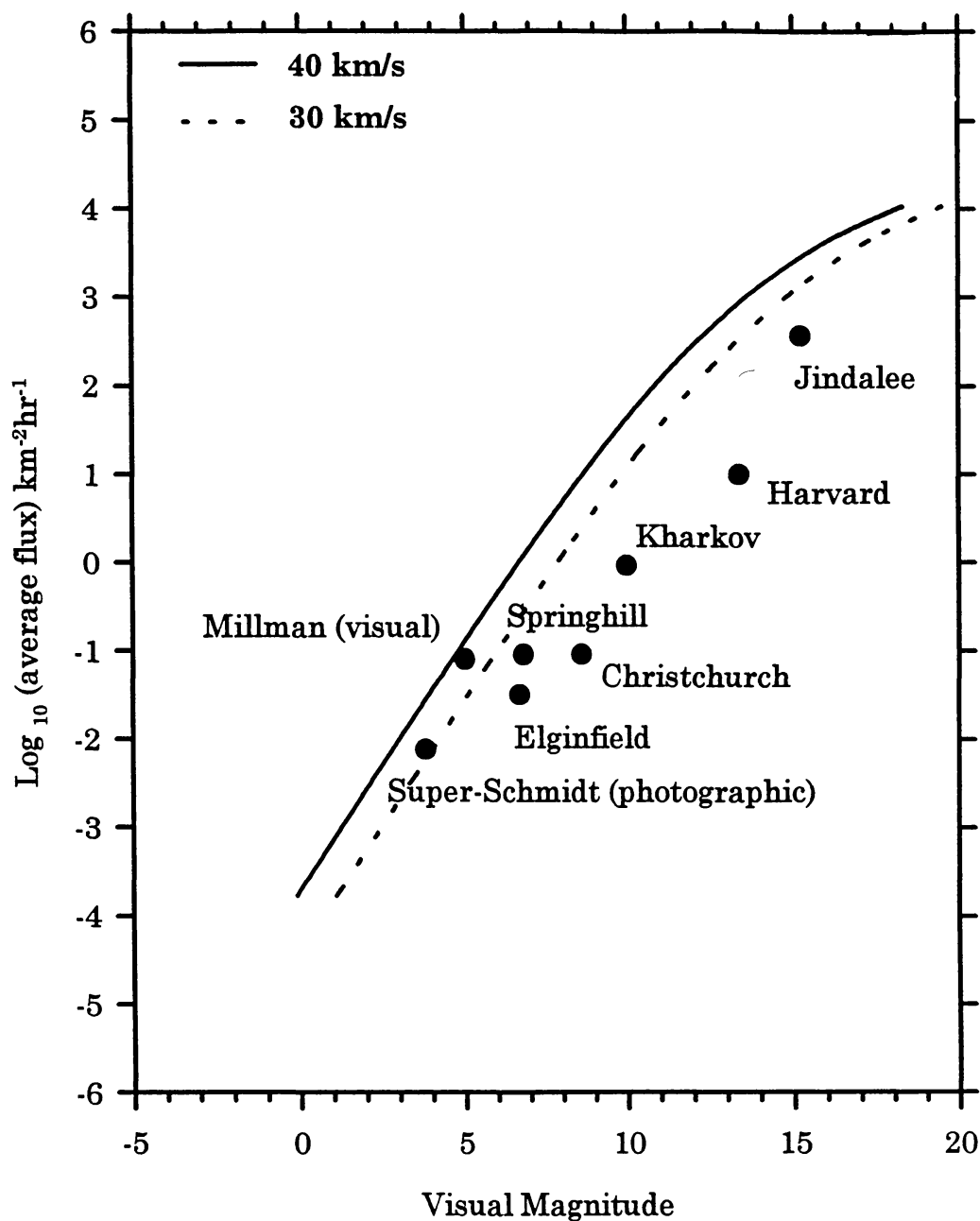
238

Figure 9. Raw (uncorrected) radar meteor flux as a function of equivalent magnitude. The lines are from Grün et al. (1985) and represent the transformation of the mass flux derived from impact experiments in space given in that reference to equivalent magnitudes for assumed velocities of 30 and 40 km/s using the magnitude-mass-velocity relations from Verniani (1973). Note the poor correspondence between the individual fluxes (labelled points) and the curves. These data points do not follow any logarithmic relation and particularly underestimate the flux at high magnitudes (small masses).
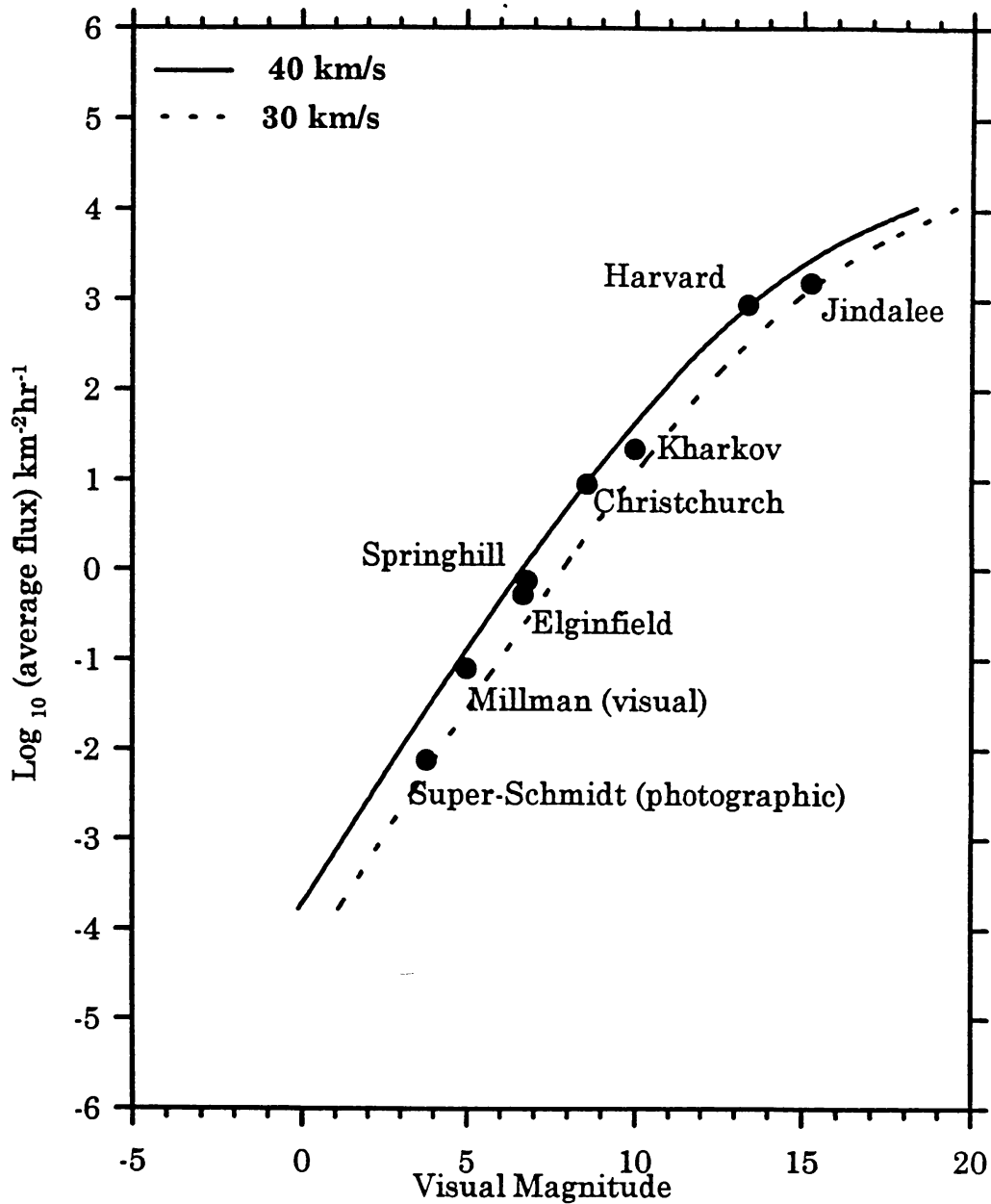
Figure 10. Corrected radar meteor flux as a function of equivalent magnitude. The lines are the same as those described in figure 9. The correspondence between the satellite derived fluxes and the radar meteor fluxes for individual radars is quite good.

radar data adequately. We note that the consistency of the individual data points with the transformed interplanetary mass distribution for a mean velocity in the 30-40 km/s suggests that this is a reasonable estimate of the mean velocity of meteors when this average is performed using magnitude as the dependent variable. To get a mean velocity distribution as a function of mass one

must debias the meteor sample as a function of velocity as the luminosity and ionization of meteors go as v^η where η is a value ~3-4 (cf. Verniani and Hawkins (1965), Jacchia et al. (1965)). As a result, the mean sporadic velocity that is obtained (about 35 km/s) represents a raw average - the true mean velocity averaged over mass is closer to 20 km/s.

4. Discussion

By removing the effects of the major showers by including them as separate sources we have been able to fit the observed rates. The final flux values for each year, for both radars for each source are given in table 2. There is an appreciable variation from year to year which may be the result of numerous atmospheric processes affecting the detectability of echoes (Elford, 1980). Very large changes in the annual detectable meteor echo flux have been observed on several occasions worldwide (McIntosh and Millman, 1964; Lindblad, 1978) leading one to suggest that a future refinement of the model would have to include prediction of the neutral atmosphere temperature profile which affects the initial train radius, rate of diffusion of the trail and also the length of the trail since the scale height changes with altitude and therefore the percentage of detectable meteor echoes. The final flux value for each year is the sum of the source fluxes divided by four. This correction accounts for the fact that the flux given for any one source is a value summed over the entire globe, but each source emanates from a specific direction (ie. not isotropic) so a stationary Earth would observe only the equivalent flux through the geometric area of the planet. It is this final value that represents the true sporadic meteoroid flux observed at Earth's orbit.

The fluxes shown in table 2 were made using the "empirical" model from the specifications for source positions and radii found in JB from the observational data. On the grounds of symmetry, one immediately recognizes that the SA and NA source are appreciably asymmetric in position relative to the apex. Indeed, the SA source is very poorly characterized in the observational data due to the limited number of orbits determined from the small southern hemisphere radar surveys.

To see if this change would make a significant difference to the derived source strengths, we ran the model again with everything kept the same except a sporadic source distribution symmetric about the apex such that each source had the mean radii of the combined pair (AH-H, NA-SA and NT-ST). The AH and H sources were placed ±70° in longitude from the apex on the ecliptic, the NT and ST were placed ±60° in latitude at the longitude of the apex while the NA and SA sources were placed ±20° in latitude also at the same sun-centred longitude as the apex. The results of this run are given in table 4. We see very little difference, in general, between the two in terms of goodness of fit as given by the σ^2 (variance of fit) values.

The new six-source model fits were also compared with the Hawkins (1957) three source model of the sporadic complex. The results of this run are given in table 5. For all years, the goodness of fit as measured by the σ^2 values is worse than either the empirical or symmetric models developed from this work. On this basis, we conclude that the derived sporadic model is a better fit to the true distribution of sporadic radio meteor radiants than Hawkins' model.

Table 6 presents the relative strengths of the sources for each model as a percentage of the total sporadic flux. We see that the AH and H sources are the strongest and the same in strength within error margins, each contributing roughly 1/3 of the total sporadic meteor population. The Toroidal components are consistently near the 5% of the total sporadic flux level for each source and are also equal in strength. It is important to recognize that these flux values are valid for the particle size range appropriate to the limiting sensitivities of the Springhill/Christchurch systems. Though the

Table 4.

Radar	Year	AH	±AH	H	±H	NT	±NT	ST	±ST
Christchurch	1960	8.61	0.56	7.77	0.64	·	·	4.67	0.24
	1963	15.3	1.21	12.3	1.18	·	·	3.55	0.45
	1964	12.1	0.74	9.82	0.89	·	·	3.88	0.33
Springhill	1959	9.16	0.54	8.07	0.55	3.36	0.22	·	·
	1960	10.3	0.62	7.13	0.64	4.73	0.25	·	·
	1963	9.09	0.60	12.2	0.66	5.47	0.22	·	·
	1964	11.1	0.53	14.4	0.54	2.91	0.22	·	·
	1965	8.61	0.46	11.6	0.47	2.76	0.19	·	·
	1966	10.6	0.46	14.8	0.65	4.89	0.35	·	·
	1967	11.7	0.59	13.9	0.71	6.50	0.34	·	·

Radar	Year	NA	±NA	SA	±SA	Total Flux	σ^2
Christchurch	1960	1.20	0.15	6.87	0.35	7.28	13.6
	1963	0.04	0.26	11.9	0.78	10.77	28.5
	1964	1.73	0.17	8.06	0.51	8.9	18.6
Springhill	1959	0.56	0.20	10.2	0.18	7.84	37.7
	1960	1.23	0.24	6.47	0.2	7.47	44.2
	1963	0.21	0.30	14.5	0.05	10.37	45.1
	1964	3.39	0.20	2.13	0.17	8.48	37.2
	1965	1.96	0.17	5.58	0.15	7.64	32.3
	1966	0.71	0.07	12.8	0.66	10.94	42.6
	1967	·	·	17.2	0.22	12.3	58.7

Table 4. Corrected flux values by source for each year data was avaliable for Christchurch and Springhill for the symmetrical sporadic source model. All fluxes are given in units of 10^{-2} km^{-2} hr^{-1}. The σ^2 column is the rms variation of the fitted rates relative to the observed rate data in units of meteors hr^{-1}. The columns headed by ± represent the error associated with the flux from a given source. The total flux is the sum of each source flux divided by four to account for the directional nature of the fluences (see text).

242

Table 5.

Radar	Year	AH	±AH	H	±H	AP	±AP	Total Flux	σ^2
Christchurch	1960	14.8	0.28	14.0	0.46	6.53	0.21	8.83	17.2
	1963	21.9	0.66	18.7	0.65	9.75	0.52	12.6	30.5
	1964	17.9	0.36	15.6	0.53	7.96	0.34	10.4	20.8
Springhill	1959	11.9	0.33	10.8	0.35	8.53	0.12	7.81	40.7
	1960	14.8	0.37	11.4	0.40	6.46	0.15	8.17	46.2
	1963	13.4	0.41	16.7	0.50	11.6	0.36	10.4	51.4
	1964	14.6	0.29	18.0	0.31	4.72	0.10	9.3	36.4
	1965	11.4	0.26	14.6	0.27	6.13	0.09	8.0	32.0
	1966	14.4	0.22	18.9	0.41	10.3	0.70	10.9	45.3
	1967	16.9	0.41	19.6	0.57	12.7	0.37	12.3	59.1

Table 5. Corrected flux values by source for each year data was avaliable for Christchurch and Springhill for the Hawkins sporadic source model. All fluxes are given in units of 10^{-2} km^{-2} hr^{-1}. The σ^2 column is the rms variation of the fitted rates relative to the observed rate data in units of meteors hr^{-1}. The columns headed by ± represent the error associated with the flux from a given source. The total flux is the sum of each source flux divided by four to account for the directional nature of the fluences (see text).

Source	Hawkins	Symmetric	Empirical
Antihelion	38 ± 6	33 ± 5	30 ± 5
Helion	40 ± 8	36 ± 9	29 ± 7
North Toroidal	–	6 ± 1	6 ± 1
South Toroidal	–	6 ± 2	6 ± 1
North Apex	–	4 ± 3	0 ± 3
South Apex	–	15 ± 7	29 ± 10
Apex	22 ± 7	–	–

Table 6. The relative strength of each source expressed as a percentage of the total sporadic meteor flux. See text for details of each model.

limiting magnitudes for these systems are roughly 2 magnitudes apart, inspection of Tables 2-4 show that the relative strength for a given year for a given common source region is generally similar between the two systems suggesting variations in strength over different masses within the sporadic particle population are gradual in this mass interval. It is also worth noting that a 2 magnitude difference at 40km/s as adopted in §3.2 corresponds to less than 1 order of magnitude in mass centred about ~5 x 10^{-5} g.

More surprising is the strong asymmetry found between the NA and SA source. In all years, the SA source is much stronger from both Springhill and Christchurch. Indeed, many years show no NA activity. There is no *a priori* reason to expect this asymmetry; variations in the showers "masked" in different years were made to attempt to alleviate this discrepancy but with no significant effect. Recent results from the Long-Duration Exposure Facility (LDEF) satellite (McBride et al., 1994) have also shown a N-S asymmetry, so this may be real. We note, however, that McBride et al. found a significantly enhanced northern flux. The raw observations from HEOS-2 (Hoffman et al., 1975) also show such an asymmetry, though the authors dismiss the result as being essentially unphysical.

5. Conclusions

The sporadic model developed in JB yields good fits to the observed sporadic meteor rate distribution gathered by radar. The AH-H sources dominate the average flux while the Toroidal component provide a minor contribution. A strong asymmetry in the strength of the apex sources is observed. The flux for each source is similar in relative strength as observed from both radar locations. The apparent fluxes determined for Springhill and Christchurch along with published flux values from other radar systems using similar sporadic distributions are in agreement with the out-of-atmosphere meteoroid fluxes measured by satellites.

6. Acknowledgements

7. References

Almond, M., 1951, The summer daytime meteor streams of 1949 and 1950. III: Computation of the orbits. *Mon. Not. R. astr. Soc.*, **111**, 37.

Babadzhanov, P.B., Bibarsov, R.S., 1992, Mass distribution of sporadic meteoroids from radar observations of overdense meteor trails, *Solar System Research*, **26**, 78.

Elford, W.G., Hawkins. G.S., Southworth, R.B., 1964, The Distribution of Sporadic Meteor Radiants, Harvard Radio Meteor Project Research Report #11, NASA, Washington, D.C.

Elford, W.G., 1980, The influence of the atmosphere on radar meteor rates, in Solid Particles in the Solar System, p. 101, eds. I. Halliday and B.A. McIntosh, Reidel, Dordrecht, Holland.

244

Ellyett, C., Keay, C.S.L., Roth, K.W., and Bennett, R.G.T., 1961, The identification of meteor showers with application to Southern hemisphere results, *Mon. Not. R. astr. Soc.*, **123**, 37.

Ellyett, C., and Keay, C.S.L., 1963, Southern hemisphere meteor rates, *Mon. Not. R. astr. Soc.*, **125**, 325.

Flemming, D.E.B., Hawkes, R.L., and Jones, J., 1993, Light curves of faint television meteors, in Meteoroids and their Parent Bodies, p.261, eds. J. Štohl and I.P. Williams, Astronomical Institute of the Slovak Academy of Sciences, Bratislava, Slovakia.

Greenhow, J.S., and Hall, J.E., 1960, The importance of initial trail radius on the apparent height and number distributions of meteor echoes *Mon. Not. R. astr. Soc.*, **121**, 183.

Grün, E., Zook, H.A., Fechtig, H., and Giese, R.H., 1985, Collisonal balance of the meteoritic complex, *Icarus*, **62**, 244.

Hawkins, G.S., 1956, A radio echo survey of sporadic radio meteor radiants, *Mon. Not. R. astr. Soc.*, **116**, 92.

Hawkins, G.S. and Upton, E.K.L., 1958, The influx rate of meteors in the Earth's atmosphere., *Ap. J.*, 128, 727

Hoffman, H-J., Fechtig, H. Grün, E, and Kissel, J., 1975, First results of the micrometeoroid experiment S 215 on the HEOS 2 satellite, *Planet. Sp. Sci.*, **23**, 215.

Jacchia, L.G., Verniani, F., and Briggs, R.E., 1967, Analysis of the atmospheric trajectories of 413 precise photographic meteors, *Smithson. Contr. Astrophys*, **10**, 1.

Jones, J., 1983, Radar observations of the Orionid meteor shower, *Mon. Not. R. astr. Soc.*, **204**, 765.

Jones, J., and Webster, A., 1992, Forward-scatter radiant mapping, in Asteroids, Comets, Meteors 1991, p. 273, eds Harris, A.W., and Bowell, E., Lunar and Planetary Institute, Houston, Texas.

Jones, J., and Brown, P., 1993, Sporadic meteor radiant distributions: orbital survey results, *Mon. Not. R. astr. Soc*, **265**, 524.

Kaiser, T.R., 1954, Theory of the meteor height distribution obtained from radio-echo observations. II - Sporadic meteors, *Mon. Not. R. astr. Soc.*, **114**, 52.

Lebedinets, V.N., 1964, Density of meteoric matter in the vicinity of the Earth's orbit from radar observations of meteors, *Soviet Astronomy*, **7**, 549.

Lindblad, B.A., 1978, Meteor radar rates, geomagnetic activity and solar wind sector structure, *Nature*, **273**, 732.

Lovell, A.C.B., 1954, <u>Meteor Astronomy</u>, Oxford University Press, London.

Mawrey, R.S., and Broadhurst, A.D., 1993, Comparison of predicted and measured detection rates of meteor signals, *Radio Sci*, **28**, 428.

McBride, N., Taylor, A.D., Green, S.F., and McDonnell, J.A.M., 1994, Asymmetries in the natural meteoroid population as sampled by LDEF, *Planet. Sp. Sci.*, (in press).

McCrosky, R.E., and Posen, A., 1961, Orbital elements of photographic meteors, *Smithson. Contr. Astrophys*, **4**, 15.

McIntosh, B.A., and Millman, P.M., 1964, Radar meteor counts: anomalous increase during 1963, *Science*, **146**, 1457.

McIntosh, B.A., 1966, The determination of meteor mass distribution from radar echo counts, *Can. J. Phys.*, **44**, 2729.

McIntosh, B.A., and Simek, M., 1980, Geminid meteor stream: structure from 20 years of radar observations, *Bull. astr. Inst. Czech.*, **31**, 39.

McKinley, D.W.R., 1961, <u>Meteor Science and Engineering</u>, McGraw-Hill, New York.

Millman, P.M., and McIntosh, B.A., 1964., Meteor radar statistics I, *Can. J. Phys.*, **42**, 1730.

Millman, P.M., and McIntosh, B.A., 1966, Meteor radar statistics II, *Can. J. Phys.*, **44**, 1593.

Neale, M.J., 1966, Radar equipment for continuous meteor observations, *Can. J. Phys.*, **44**, 1021.

Olsson-Steel, D., and Elford, W.G., 1986, The height distribution of radio meteors: observations at 2 MHz, *J. atmos. terr. Phys.*., **49**, 243.

Štohl, J., 1968, Seasonal variation in the radiant distribution of meteors, in <u>Physics and Dynamics of Meteors</u>, p. 298, eds. L. Kresak and P.M. Millman. Reidel, Dordrecht, Holland.

Thomas, R.M, Whitham, P.S., and Elford, W.G., 1988, Response of high frequency radar to meteor backscatter, *J. atmos. terr. Phys.*, **50**, 703.

Verniani, F., and Hawkins, G., 1964, On the ionizing efficiency of meteors, Harvard Radio Meteor Project Research Report #5, NASA, Washington,   D.C.

Verniani, F., 1966, Meteor masses and luminosity, *Smithsonian Astrophysical Observatory Research in Space Sciences*, **219**, 1.

Verniani, F., 1973, An analysis of the physical parameters of 5759 faint radio meteors, *J. Geophys. Res.*, **76**, 8429.